Behavior of Plasmons in an Amorphous Silicon-Carbon Alloy System Studied by X-Ray Photoelectron Spectroscopy

Yoshifumi Katayama, Toshikazu Shimada, and Katsuhisa Usami[a]
Central Research Laboratory, Hitachi, Ltd., Kokubunji, Tokyo 185, Japan
(Received 9 December 1980)

Valence-electron plasmons in an amorphous silicon-carbon alloy system a-$Si_x C_{1-x}$:H ($0 \leq x \leq 1.0$) are observed as the satellites of core-electron levels in the x-ray photoemission spectra. The atomic density of a-$Si_x C_{1-x}$:H as a function of x is determined from the valence-electron density n_v obtained from observed plasmon energy $\hbar\omega_p$ with use of $\hbar\omega_p = \hbar[(4\pi e^2/m)n_v]^{1/2}$ and the results of thermal effusion experiments. The results are discussed in relation to the coordination of carbon atoms in a-$Si_x C_{1-x}$:H.

PACS numbers: 71.45.Gm, 71.25.Mg, 79.60.Eq

Hydrogenated amorphous silicon a-Si:H has attracted a great deal of attention not only as a potential material for solar cells[1] and imaging devices[2,3] but also as a good system for the study of amorphous materials.[4] For both purposes, the interest has extended to the hydrogenated amorphous alloys of different group-IV elements with controlled optical and electrical properties and increased thermal and chemical stabilities.[5-8] The hydrogenated silicon-carbon alloys a-Si_xC_{1-x}:H provide particularly good systems for such studies because of their specific electronic structure and chemical bonding.

The plasmon energy $\hbar\omega_p$ is given, to the first approximation, as $\hbar\omega_p = \hbar[(4\pi e^2/m)n_v]^{1/2}$, where n_v is the valence-electron density.[9] In a-Si_xC_{1-x}:H, n_v increases with increasing carbon content because the covalent radius of carbon is smaller than that of silicon. This Letter describes the behavior of valence-electron plasmons observed as satellites of core-electron levels in the x-ray photoemission spectroscopy (XPS) spectra. The results are discussed in relation to the coordination of carbon atoms in a-Si_xC_{1-x}:H.

Specimens were prepared by diode-type reactive sputtering. High-purity polycrystalline silicon and graphite targets were simultaneously sputtered in a purified Ar-H_2 gas mixture. Crystalline silicon wafer substrates were used. The microscopic homogeneity of the specimens was confirmed by XPS and infrared absorption measurements. Details of sample characterization, including determination of the alloy composition x and of the optical gap, have been reported elsewhere.[7,10]

Samples were transferred from the sample preparation chamber to the XPS vacuum chamber within 10 min. This maintained sample surfaces under a close to *in situ* condition. A Vacuum Generators ESCA-3 system was used to take the XPS spectra. The Mg $K\alpha$ line was used for photoelectron excitation.

In the XPS spectra, valence-electron plasmon emission satellite peaks associated with the Si 2*s*, Si 2*p*, and C 1*s* core levels were observed. Figure 1 shows the XPS spectra of a-Si_xC_{1-x}:H for various compositions x near the Si 2*p* core level in the energy scale, where the Si 2*p* levels are taken to be the origin of the energy. The peak position $\hbar\omega_p$ and the full width at half maximum (FWHM) are plotted as a function of x in Figs. 2(a) and 2(b). For reference, the $\hbar\omega_p$ and the FWHM measured under the same conditions for diamond, graphite, cubic crystalline SiC, and crystalline Si (i.e., compounds with four valence electrons belonging to each carbon or silicon

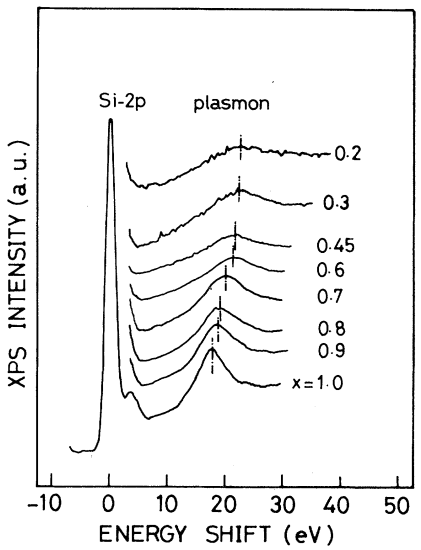

FIG. 1. XPS spectra of a-$Si_x C_{1-x}$:H in the energy range near the Si 2*p* level. The Si 2*p* core level is taken to be the origin of the energy scale.

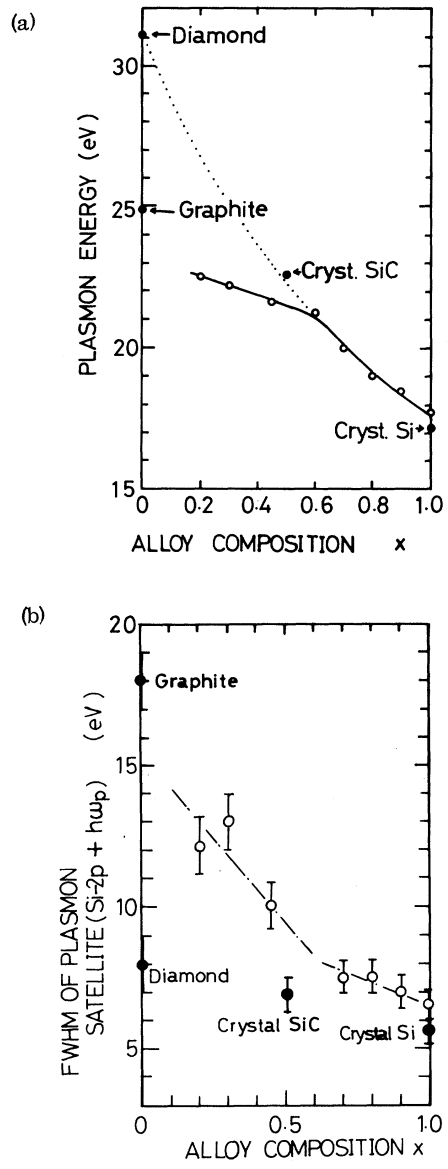

FIG. 2. (a) The plasmon energy $\hbar\omega_p$ and (b) the FWHM of plasmon satellites vs alloy composition x.

atom) are shown as the solid circles.

In the region $x = 1.0$–0.6 (i.e., silicon-rich region), $\hbar\omega_p$ in a-Si_xC_{1-x}:H falls on the curve connecting the plasmon energies of the crystalline silicon, cubic SiC, and diamond. In the region of $x < 0.6$ (carbon-rich region), it deviates from this curve and approaches the value for graphite. The curve of the FWHM versus x exhibits a similar trend. It should be noted that the increase in the FWHM in the carbon-rich region is not due to inhomogeneity in the a-Si_xC_{1-x}:H films. As reported

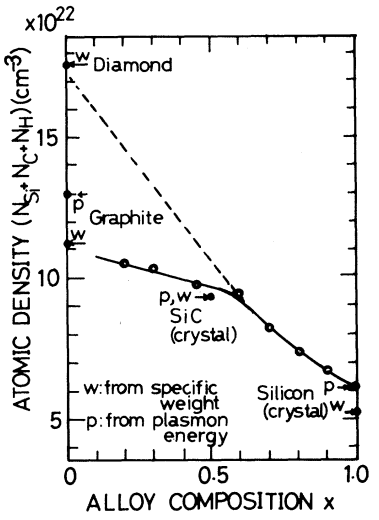

FIG. 3. Atomic density of a-$Si_x C_{1-x}$:H determined with use of the plasmon energy $\hbar\omega_p$ and results of the thermal evolution experiment.

elsewhere,[7,10] the microscopic homogeneity has been confirmed by XPS and infrared absorption measurements. For example, the binding energy of the Si $2p$ core electrons decreases monotonically as x increases while the linewidth of the Si $2p$ core levels remains almost constant. Therefore, it is quite possible that the sudden increase in the width of the plasmon loss line indicates the existence of another channel of plasmon damping.

As stated previously, the plasmon energy $\hbar\omega_p$ is related to the valence-electron density n_v by $\hbar\omega_p = \hbar(4\pi e^2 n_v/m)^{1/2}$, where m is the free-electron mass. It is known that in materials with simple band structures and in cases when $\hbar\omega_p$ is large compared with interband energies, the free-electron mass is used in the formula for the plasma.[9] Therefore, an approximate valence-electron density n_v may be obtained from the observed plasmon energy $\hbar\omega_p$.

Each carbon and silicon atom donates four valence electrons, and hydrogen atom gives one valence electron. That is,

$$n_v = 4N_C + 4N_{Si} + N_H,$$

where N_C, N_{Si}, and N_H are the atomic densities of C, Si, and H atoms in a-Si_xC_{1-x}:H, respectively. N_H can be determined independently by thermal evolution experiment.[7] Thus, with use of simple arithmetic $N_C + N_{Si} + N_H = \frac{1}{4}(n_v - N_H) + N_H$, the total atomic density $(N_C + N_{Si} + N_H)$ can be plotted as a function of x as shown in Fig. 3. For comparison, the atomic densities of crystal Si,

SiC, diamond, and graphite are also shown. The atomic density obtained here reflects the local structure of amorphous network more directly than that determined from the macroscopic mass density which is averaged over an amorphous film; this quantity may be considered a useful measure in discussions of chemical bonding. In Fig. 3, the atomic density of a-Si_xC_{1-x}:H deviates from the curve connecting the atomic densities of crystal Si and diamond at $x \sim 0.6$ and approaches that of graphite at $x = 0$. This seems to imply a drastic change in the chemical-bonding states in a-Si_xC_{1-x}:H. In addition, the FWHM of plasmon satellites is greatly enhanced in the same carbon-rich region, as seen in Fig. 2(b).

Although the position of $\hbar\omega_p$ is displaced to the higher-energy side with increasing wave vector q, [11] the width of the plasmon satellites observed in the XPS spectra does not show the effect of dispersion because of q^{-2} weighting in the cross section.[12] As previously stated, inhomogeneity in the film is not the main cause of the width. Therefore, the observed increase in the plasmon width with increasing carbon content is considered to be due to an increase in plasmon damping. The damping of the valence-electron plasmons with small wave vector q is thought of as being mainly determined by single-particle excitations such as interband transitions via electron-electron interactions.[9] Furthermore, it is seen in Fig. 2(b) that the width of plasmon satellites increases more rapidly at $x < 0.5$ with decreasing x and approaches the value not of diamond but of graphite at $x = 0$. This increase is not due to the inhomogeneity in the films as described above. Therefore, it is probable that another mechanism of plasma damping, which is relevant to the plasmon damping in graphite, due to single-particle excitations via π-electron bands of threefold-coordinated carbon atoms also contributes at $x < 0.5$.

As previously reported, the optical gap of reactively sputtered a-Si_xC_{1-x}:H reaches a maximum near $x = 0.6$.[7] For $x > 0.6$ (i.e., silicon-rich region), the optical edge shifts toward the higher-energy side as x decreases, while for $x < 0.6$ (carbon-rich region) the optical gap decreases as x decreases. This is a result of a decrease in the gradient of the $(\alpha h\nu)^{1/2}$ vs $h\nu$ plot. This feature favors diamondlike fourfold coordination in the silicon-rich region and graphitelike threefold coordination in the carbon-rich region.

The optical gap E_0 and the plasmon energy $\hbar\omega_p$ are quantities determined mainly by valence electrons which reflect the electronic structure averaged over several atomic spacings. On the other hand, the chemical shifts in the C 1s, Si 2s, and Si 2p core levels in a-Si_xC_{1-x}:H observed by XPS measurements were examined as quantities which reflect more local environments. The binding energy of the C 1s level drawn as a function of x has a break at $x \sim 0.6$,[10] where anomalies were found in the optical gap E_0 and the plasmon energy $\hbar\omega_p$ as described above, while the binding energy of Si 2p level is a smooth function of x. The amount of chemical shift in the Si 2p level can be understood by considering the electronegativity difference between silicon (1.8) and carbon (2.5). The fact that the C 1s binding energy versus x curve has different slopes on both sides of $x = 0.5$–0.6 probably shows that some drastic change occurs in the carbon-atom environments.

Thermal evolution measurements also provide a similar break in the x dependence.[7] The hydrogen evolution temperature at which the greatest amount of hydrogen evolves from a-Si_xC_{1-x}:H alloy films during 15 min of isothermal annealing in a vacuum with 100 deg interval increased as x decreased for $x > 0.6$ and became flat for $x < 0.5$. This fact seems to show that the nature of the chemical bond between hydrogen atoms and silicon or carbon atoms changes at $x \sim 0.5$.

In summary, the alloy-composition dependences of both the quantities reflecting electronic structure averaged over several atomic spacings (i.e., the atomic density and optical gap) and the quantities reflecting more local environments (i.e., the chemical shifts of core-electron levels and the hydrogen evolution temperature) have similar breaks at an alloy composition of $x = 0.5$–0.6. All of these characteristics seem to originate from the same change in chemical-bonding structure in a-Si_xC_{1-x}:H alloy films.

The authors are grateful to Dr. Yasuhiro Shiraki, Dr. Keisuke L. I. Kobayashi, and Dr. Yoshimasa Murayama for their participation in many valuable discussions. We also would like to thank the staff of the Material Analysis Center at Central Research Laboratory, Hitachi, Ltd., for their help with the hydrogen evolution experiments.

[a]Present address: Hitachi Research Laboratory, Hitachi, Ltd., Hitachi, Ibaraki-ken, Japan.

[1]D. E. Carlson and C. R. Wronski, Appl. Phys. Lett.

28, 671 (1976).
[2]Y. Imamura, S. Ataka, Y. Takasaki, C. Kusano, T. Hirai, and E. Maruyama, Appl. Phys. Lett. 35, 349 (1979).
[3]I. Shimizu, T. Komatsu, K. Saito, and E. Inoue, J. Non-Cryst. Solids 35-36, 773 (1980).
[4]For example, N. F. Mott and E. A. Davis, *Electronic Processes in Non-Crystalline Materials* (Clarendon, Oxford, 1979), p. 320.
[5]D. A. Anderson and W. E. Spear, Philos. Mag. 35, 1 (1977).
[6]J. Chevallier, H. Wieder, A. Onton, and R. Guarnier, Solid State Commun. 24, 867 (1977); A. Onton, H. Wieder, J. Chevallier, and C. R. Guarnier, *Amorphous and Liquid Semiconductors*, edited by W. E. Spear (The Centre for Industrial Consultancy and Liaison, University of Edinburgh, Edinburgh, 1977), p. 357.
[7]T. Shimada, Y. Katayama, and K. F. Komatsubara, J. Appl. Phys. 50, 5530 (1979).
[8]H. Wieder, M. Cardona, and C. R. Guarnier, Phys. Status Solidi (b) 92, 99 (1979).
[9]For example, P. M. Platzman and P. A. Wolff, *Waves and Interactions in Solid State Plasmas* (Academic, New York, 1973).
[10]Y. Katayama, K. Usami, and T. Shimada, to be published.
[11]P. G. Gibbons, S. E. Schnatterly, J. J. Ritsko, and J. R. Fields, Phys. Rev. B 13, 2451 (1976).
[12]R. J. Baird, C. S. Fadley, S. M. Goldberg, P. J. Feibelman, and M. Šunjić, Surf. Sci. 72, 495 (1978).

Two-Dimensional Resistivity of Ultrathin Metal Films

R. S. Markiewicz[a] and L. A. Harris
General Electric Research and Development Center, Schenectady, New York 12301
(Received 20 November 1980)

Extremely thin (monolayer to 100 Å) continuous metallic films of Pt can be formed on Si substrates. In the thinnest films the conductance is found to be $S = S_0 + \alpha^1(e^2/\pi^2\hbar)\ln T + \delta T^2$, with $\alpha^1 = 0.75 \pm 0.15$ from liquid-He temperatures up to $T \geq 390$ K. Thicker films show a transition as a function of temperature from two- to three-dimensional behavior, with a corresponding resistivity minimum. The negative magnetoresistance is in good agreement with predictions of localization theory.

PACS numbers: 71.55.Jv, 72.15.Qm, 73.60.Dt

Recent theories of conductivity in reduced dimensions[1-3] have predicted that sufficiently fine wires and thin films do not display ordinary metallic conductivity. Instead, the resistance increases with decreasing temperature and diverges as $T \to 0$, with $R \propto \ln T$ in two dimensions and $R \propto 1/T^{1/2}$ in one dimension. These dependences have now been observed at low temperatures ($T \leq 10$ K) in a number of systems.[4-7] However, agreement with theory is far from complete. For instance, the criterion for the observation of lower-dimensional effects is that the sample thickness (or diameter) be less than the Thouless length L_T, where the various theories estimate $L_T^2 = 2l_e l_i$ (localization theory[1,2]) or $L_T^2 = 4D\hbar/k_B T$ (many-electron theory[3]), where l_e (l_i) is the elastic (inelastic) scattering length, $D = l_e v_F/2$ is the two-dimensional diffusion constant, and v_F is the Fermi velocity. Experiments[4,7] find that l_i is orders of magnitude smaller than expected. Furthermore, one-dimensional resistivity has only been observed[7] in relatively dirty materials (alloys with enough impurity scattering that $\partial\rho/\partial T$ is weak or negative even in bulk samples)[8,9] with diameter $d \leq 1700$ Å; all experiments[9,10] to date on clean metal wires have failed to observe localization, down to $d = 200$ Å. This is contrary to theory, which predicts a larger Thouless length in a cleaner metal (longer mean free path).

We present here the results of our study of conductivity in ultrathin (monolayer to 100 Å), continuous Pt films. These results are significant for a number of reasons: (1) They present the first observation of localization effects in clean metal films. In agreement with the null results of Overcash *et al.*[9] and Garland, Gully, and Tanner,[10] localization is only observed in film less than 100 Å thick. (2) The logarithmic slope approximately agrees with values measured in Si inversion layers.[5,11] Considering that carrier densities in these two systems differ by several orders of magnitude, this constitutes an impressive verification of the universality of the effect. (3) Monolayer films show localized behavior up to room temperature—twenty times higher than

